University of Huddersfield Repository

Kollar, László E. and Farzaneh, Masoud

Modeling Sudden Ice Shedding from Conductor Bundles

Original Citation

Kollar, László E. and Farzaneh, Masoud (2012) Modeling Sudden Ice Shedding from Conductor Bundles. IEEE Transactions on Power Delivery, 28 (2). pp. 604-611. ISSN 0885-8977

This version is available at http://eprints.hud.ac.uk/id/eprint/15999/

http://eprints.hud.ac.uk/

Modeling Sudden Ice Shedding from Conductor Bundles

László E. Kollár, and Masoud Farzaneh, *Fellow, IEEE*

Abstract—**Sudden ice shedding from conductor bundles was modeled numerically and experimentally by improving the approaches proposed formerly for a single cable. The experimental study was carried out on a small-scale laboratory model of one span of a twin bundle. A numerical model of the experimental set-up was developed using the commercial finite element software ADINA. This model was validated by simulating (i) the vertical cable vibration during load shedding tests on a full-scale line of single conductors [1]; (ii) the bundle rotation on a full-scale twin bundle during static torsional tests [2]; and (iii) the vertical cable vibration and bundle rotation at mid-span during the present load shedding tests on a small-scale twin bundle. The coincidence of calculated and measured tendencies justified the applicability of the numerical model to simulate the vibration following ice shedding from bundled conductors in most cases. The model was finally applied to simulate sudden ice shedding from a full-scale span with a twin bundle. Simulation results showed that the application of spacers reduces the cable jump height during this vibration; however, a higher number of spacers in the same span does not decrease the angle of bundle rotation**.

Index Terms—**bundle rotation, cable vibration, ice shedding, numerical modeling, small-scale experiment.**

I. INTRODUCTION

SHEDDING of the ice accreted on transmission line cables is a recurrent problem in cold regions. The falling of large ice chunks results in high-amplitude vibration of the de-iced cable giving rise to important dynamic forces acting on the transmission line. When a subconductor in a multiconductor bundle sheds, the rotation of the bundle may also be significant, leading to bundle collapse in extreme cases. Bundle collapse occurs when the bundle rotation exceeds a critical angle so that the bundle loses its stability and does not untwist itself after load removal [2], [3]. A review of ice-related dynamic problems on overhead lines, including ice shedding and bundle rolling is provided in [4].

Research efforts to understand and simulate the dynamic effects of ice shedding have been carried on for several decades. Reference [1] modeled ice shedding experimentally

L. E. Kollár and M. Farzaneh are respectively member and chairholder of the NSERC/Hydro-Quebec/UQAC Industrial Chair on Atmospheric Icing of Power Network Equipment (CIGELE) and Canada Research Chair on Atmospheric Icing Engineering of Power Networks (INGIVRE), http://www.cigele.ca, International Research Center on Atmospheric Icing and Power Network Engineering (CENGIVRE), University of Quebec at Chicoutimi, 555 boulevard de l'Université, Chicoutimi, Quebec, Canada, G7H 2B1 (e-mail: laszlo_kollar@uqac.ca and farzaneh@uqac.ca).

by load-dropping tests and observed the resulting cable jump. Ice shedding from a two-span section was modeled numerically in [5] using the commercial finite-element analysis software ADINA [6], and model predictions were validated on a small-scale laboratory model. Reference [7] studied the effects of ice thickness, partial shedding, and different line parameters on the dynamic response of ice shedding on transmission lines by a similar numerical approach. Conductor vibration following ice shedding from one subconductor in a bundle was simulated numerically by [8]. A different modeling approach was applied in [9] to examine the dynamic behavior of a spacer damper located at mid-span in twin, triple and quad bundles after ice shedding.

The present study aims to simulate both numerically and experimentally ice shedding from conductor bundles, and to predict how cable jump and bundle rotation depend on the number of spacers in one span. The finite element model of [8] is improved so as to (i) predict transverse cable motion, and consequently bundle rotation, (ii) simulate shedding of concentrated loads as it occurs in experimental modeling of ice shedding, and (iii) consider cable damping in a different way providing more realistic results. The experimental simulation is implemented by load shedding tests on a small-scale laboratory model based on ideas proposed in [1] and [5], and extending them to bundled conductors. Numerical model predictions are validated by comparing them to observations obtained during these experiments as well as during former full-scale tests. Finally, the model is applied to simulate sudden ice shedding from a subconductor in a full-scale twin bundle.

II. EXPERIMENTAL SET-UP

The experimental set-up was constructed for modeling one span of a twin bundle with spacers in the horizontal plane. The distance between the cables was 5 cm. Two identical Vanguard 7x19 construction stainless steel cables were connected at each end to aluminum plates hinged to the suspensions. Cables with two different diameters were used in different tests; their parameters are provided in Table 1. The span length was limited to 6.4 m, because of the laboratory chamber size. In the set-up, simple bars acted as spacers, satisfactorily modeling the spacers' role of maintaining a constant distance between the subconductors. However, the bars could not simulate the damping effects of the spacers. Experiments were carried out with up to five spacers. Although sub-span lengths are usually

Parameter	Unit	Vanguard 1/8''	Vanguard 3/16''
Cable diameter	(mm)	3.2	4.8
Cross-sectional area of the cable (sum of strand cross-sections)	(mm^2)	5.50	12.33
Mass per unit length of the cable	(kg/m)	0.043	0.097
Sag of unloaded cable	(m)	0.290	0.309

unequal in practice, equal sub-span lengths were applied in these tests for the sake of simplicity. A spacer was fixed at mid-span when there was an odd number of spacers along the span (one, three or five), whereas there was no spacer at mid-span with an even number of spacers (two or four).

The stress-strain curves of the cables were determined in tensile tests carried out according to the ASTM SA-370 Standard [10] by using an MTS material test machine. The elongation of the sample was measured by an extensometer fixed to the cable. Fig. 1 illustrates the set-up at the beginning of a tensile test. The deformation rate was kept at $5 \cdot 10^{-4}$ 1/s, which meant a displacement rate of approximately 6 mm/min with 200-mm long samples. Measurements were repeated with two to three samples of the same diameter, and stress-strain curves were approximated by piecewise linear relationships. These relationships are shown in Fig. 2, and they served as input when defining cable material properties in the numerical model.

The ice load was modeled by weights attached to the cables via electromagnets manufactured by AEC Magnetics. Eight weights of 0.812 kg each were attached to both cables with approximately constant distances in between, representing a load of 8 times 0.812 kg in 6.4 m, i.e. 1.015 kg/m. The current in the electromagnets was switched on before the weights were attached, meaning that switching off the current released the weights thereby simulating ice shedding from the corresponding area of the cable. When simulating sudden shedding from the whole span, the eight weights on either cable were released at the same time. The main elements of the experimental set-up are shown in Fig. 3.

The time history of vertical displacement of cables following load shedding was observed at mid-span by fixing a scale behind the cables and recording cable movement by a Panasonic digital video camcorder (model no. PV-GS400). The distance between the cable and the scale was significantly less than that between the cable and the camera. Thus, the error in the cable position as viewed by the camera was less than the measurement error, i.e. the discrepancy between the displacement peaks as obtained in two measurements under the same conditions. The angle of bundle rotation was also determined at mid-span by using the horizontal and vertical coordinates of the spacer attachment points. In order to achieve this goal, a scale was placed horizontally above the cables, another scale was fixed vertically near the cables, and
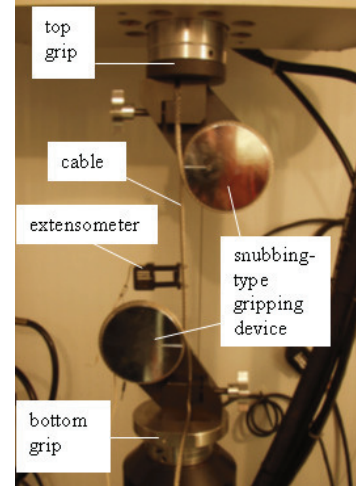
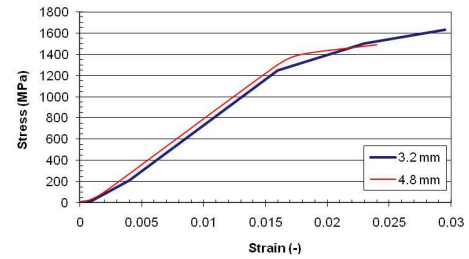

Fig. 1. Setup for cable tensile tests

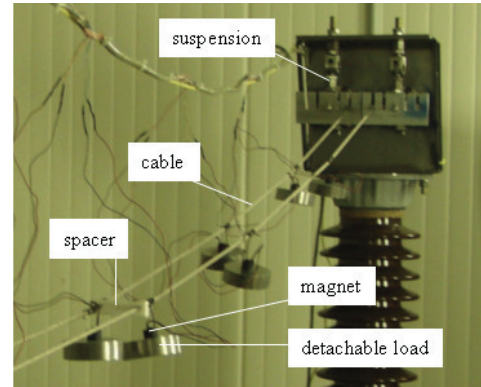Fig. 2. Stress-strain curves of Vanguard stainless steel 7x19 cables with two different diameters

Fig. 3. Part of the experimental setup showing the main elements

the vibration was recorded by the same camera. Coordinates of the spacer attachment points were given by the pixel numbers in the video recording, and the scales were used to calibrate the pixel size. The highest jump was occurring at mid-span when there was no spacer there, so that a vertical vibration was observed in the configurations without spacers (i.e. single cable), and with two and four spacers. However, since bundle rotation was measured at mid-span by using the spacer attachment points, bundle rotation was observed when applying one, three or five spacers, one of them located at mid-span.

The model scale factor can be determined from the ratio of the dynamic elasticity of a real conductor to that of the model

conductor [11]. According to this definition, the scale factor of the present model is quite small (around 7), which means that the span length of the corresponding full-scale line (approximately 45 m) is significantly shorter than those used in practice. Therefore, the numerical model presented in Section III will also be applied to a full-scale line with a longer span length in order to observe tendencies as to how cable jump height and bundle rotation vary with the number of spacers in the span, or in other words, with sub-span length.

III. NUMERICAL MODELING

In this section, the model for a single span of bundled conductors is presented. This model was developed using the finite-element analysis software ADINA [6]. The cable model is based on [5] and [7]; whereas the model of cable damping is the one proposed in [12]. A simple model for suspension is developed in this section. The present authors already proposed spacer models in previous research [8], [9], [13]. However, a simplified version of these models is considered here, which satisfactorily simulates the behavior of the rigid spacers used in the experiments. In the present experiments, as in those of [1], ice shedding is modeled by load shedding. The numerical model simulating this process is presented at the end of this section.

A. Cable

The cable is modeled by two-node isoparametric truss elements with large kinematics. A constant initial pre-strain corresponding to the installation conditions is prescribed as an initial condition for all cable elements [5], [7]. This initial strain may be obtained once the horizontal tension in static equilibrium of the catenary and cable geometrical and material properties are known [14]. The material properties of the cable are accounted for by a nonlinear elastic material model, not allowing compression and defining a piecewise linear stress-strain curve. This stress-strain relationship is based on tensile tests when modeling the experimental set-up, and on the data provided in literature when modeling full-scale transmission lines. The mesh contains 100 cable elements in each subconductor.

Cable damping is modeled by Rayleigh damping following the proposition of [12]. In this case the Rayleigh damping parameters were obtained from the natural circular frequencies and damping ratios in two different vibration modes [15]. The natural circular frequencies were determined from the linear theory of free vibration of suspended cables [16]. The damping ratios were calculated from the logarithmic decrement which was obtained following the observation of the decay of vertical cable vibration. The damping ratio of Vanguard cables used in the laboratory experiments was obtained as 0.02.

B. Suspension

The subconductors in the experimental set-up are connected to an aluminum element which is hinged to the suspension. This aluminum element is modeled by one truss element at each cable attachment with a simplification of its geometry obtained by defining a uniform area of cross section. This element is associated with elastic isotropic material representing aluminum. Rotation around the transverse axis is allowed at the points where the cable is attached to the aluminum element, and where the latter is hinged to the suspension.

C. Spacer

A simple spacer model was proposed in [13], and later improved in [8] by including a more complex geometry, as well as the flexibility and damping properties of the spacer damper. A further improvement occurred in [9] where the spacer damper properties were determined more precisely in material tests. When modeling the present small-scale experiments and the torsional tests of [2], a simplification is applied, since rigid spacers were used in most of these experiments. In one case, a friction spacer was used, which is an in house design, and the data needed for developing its more sophisticated model were not reported in [2]. This simplified model is summarized briefly as follows.

Spacers for a twin bundle are considered as simple rods clamped to a conductor at each end [8]. They are modeled by two-node truss elements in the load shedding tests and by beam elements in the torsional tests, and are associated with an isotropic linear elastic material. In the dynamic load shedding tests, the structural damping of spacers is considered by a nonlinear spring element with exponent 1 and with a damping constant calculated from

$$c_s = 2\zeta_s \sqrt{E_s A_s m_s}$$

where ζ_s is the spacer damping ratio (which was set at 0.005 when simulating the small-scale experiments) , E_s is the Young's modulus, and A_s and m_s are the cross section and mass per unit length of the spacer element, respectively.

D. Ice Load and Ice Shedding

Ice usually appears on transmission line cables as a distributed load. Since distributed loads cannot be applied on truss elements, Reference [7] proposed a model that took the ice load into account by increasing the cable density proportionally with the ice load weight in the static analysis. Then, the density of the ice-shedding subconductor was decreased in the dynamic analysis; and this abrupt change in density, and correspondingly in the mass matrix, simulated the effects of sudden ice shedding.

This study considers ice load and shedding in a different manner that better approximates the load shedding tests presented in Section II and those reported in [1]. The attached discs apply concentrated loads on the cable, so that this model considers the load resulting from several point loads along the cable. If these concentrated loads are attached to many points of the cable, they provide a satisfactory approximation of the distributed ice load. Thus, in the static analysis concentrated loads are applied along the span at constant distances similarly to the experiments. Then, these loads are removed at the

beginning of the dynamic analysis simulating sudden shedding. This model is applied to simulate uniformly distributed ice along the conductor with the same initial ice mass on each subconductor. However, it can easily be adapted to simulate non-uniform ice accumulation and different ice masses on the subconductors by varying the concentrated loads.

IV. VALIDATION OF NUMERICAL MODEL

A. Sudden Load Shedding on a Full-Scale Line of Single Conductors

The numerical model is first validated by comparisons to full-scale observations. Due to the lack of data on sudden ice shedding tests or field observations on full-scale conductor bundles, the numerical model was applied to simulate ice shedding tests on a full-scale line of single conductors as well as static torsional tests on a full-scale span of a twin bundle. These tests had already been carried out and the results are available in [1] and in [2], respectively.

The numerical model is applied to simulate vertical cable vibration following the sudden release of loads on a full-scale five-span section of single conductors. The measured and computed sags of the loaded span in static equilibrium and the conductor jump heights are compared. The results of the original load shedding tests were reported in [1]. The five-span section is located on an inclined surface where the altitude differences between the suspension points of each span beginning from the leftmost span are 5, 16, 28, 16 and 8 m. The corresponding span lengths are 283, 387, 247, 213 and 309 m, respectively. Reference [1] worked with three different suspension arrangements and carried out several shedding scenarios, of which four were repeated numerically for the present comparison: suspension with standard suspension string and full shedding from the middle span with loads of 1.49, 2.98, 4.47 and 5.96 kg/m (1, 2, 3 and 4 lb/ft). The loads were attached at every 6.1 m (20 ft) in the experiments. One span was divided into 100 elements in the numerical model, and concentrated loads were applied at every second points, i.e. at every 4.94 m. Thus, the distance between two point loads were not exactly the same as in the experiment, but the total load was the same. The conductors were made of copper-equivalent steel-cored aluminum whose data are provided in Table 2. Its stress-strain curve was considered linear for positive strains with Young's modulus of 91.8 GPa, and no compression was allowed. Dead ends were assumed at the extreme suspensions, whereas at the other suspensions the only free degree of freedom was the rotation around the horizontal axis perpendicular to the plane determined by the suspension and the connecting cables. One time history of vertical conductor oscillation was shown in [1], which was used to approximate the logarithmic decrement and to estimate the damping ratio of the cable as $\zeta = 0.03$.

The sags of the loaded span in the static equilibrium and the conductor jumps above the loaded position after shedding are shown in Figs. 4a and 4b, respectively. These figures support the reliability of the model for dynamic analysis of full-scale

TABLE II
PARAMETERS OF COPPER-EQUIVALENT STEEL-CORED ALUMINUM, 795 MCM ACSR 26x7 AND BERSFORT ACSR CONDUCTORS

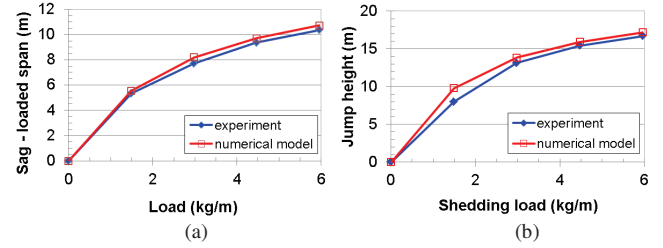| Parameter	Unit	Copper-eq. steel-cored Al	795 MCM ACSR (26 x 7)	Bersfort ACSR
Cable diameter	(mm)	19.6	28.2	35.6
Cross-sectional area of the cable (sum of strand cross-sections)	(mm^2)	227.6	460	747.1
Mass per unit length of the cable	(kg/m)	0.85	1.628	2.37
Sag of unloaded cable	(m)	5.18	3.34	6.0

Fig. 4. Simulation of load shedding tests on a full-scale five-span section with single conductors; experimental results were reported in [1]; (a) static sag of the loaded span, (b) conductor jump height above loaded position

transmission lines. The only considerable overestimation of the model, by 22%, appears for the jump height after the shedding of the 1.49 kg/m load. In all other cases, the overestimation was in the range of 3-6%. The period of vibration was reported at 4.12 – 4.16 s in [1], whereas it occurred at 4.2 s for the 1.49 kg/m load and then reduced to 3.6 s for higher loads according to numerical calculations. Since the original experiments were carried out with single conductors, these comparisons cannot validate how the model predicts bundle rotation in a full-scale line during vibration.

B. Torsional Tests on a Full-Scale Span with a Twin Bundle

In order to evaluate the model concerning bundle rotation in full-scale transmission lines, some of the static torsional tests of [2], were also simulated numerically. They applied a torque on twin and quad bundles until the bundle collapsed. They varied the span length, the subconductor spacing, the number, location and type of spacers, and the conductor tension. Two of these tests were repeated numerically: Tests No. 21 and No. 58 in [2], because the complete moment-rotation curves were presented for these cases. These tests were conducted on a horizontal arrangement of a twin bundle with one spacer at mid-span, and with three spacers at ¼, ½ and ¾ of the span. The span length was 244 m, and the subconductor spacing was 0.457 m. The conductor type was 795 MCM ACSR (26 x 7) whose data are provided in Table 2. The stress-strain curve of conductors in the model was considered linear for positive strains with a Young's modulus value of 75.1 GPa, and no compression was allowed. The moment was applied at mid-span. Rotation around the axis perpendicular to the vertical plane of the conductor in static equilibrium was allowed at the suspension, and further degrees of freedom were fixed.
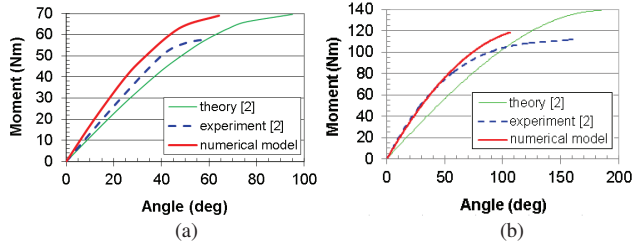
Fig. 5. Simulation of static torsional tests on twin bundles; experimental results were reported and theory was proposed in [2]; (a) one spacer at mid-span, (b) three spacers at ¼, ½ and ¾ span

The moment-bundle rotation relationships are shown in Fig. 5. When one spacer is applied (Fig. 5a), the model overestimates the measured moments, and consequently, the collapse moment by about 20%. The theory presented in [2] underestimates the measured moments to a similar extent, up to 45°, then the two curves approach each other, and the collapse moment and collapse angle are overestimated. The numerical model provides a significantly closer estimation of the collapse angle than this theory. The discrepancy between the experimentally and numerically obtained curves for three spacers (Fig. 5b) is different from that for one spacer (Fig. 5a), which may be due to the different methods as how the moment was applied in the experiments or due to the different spacer types used in the experiments. The estimation of the numerical model is excellent, the two curves coincide, up to 50°. Then, the numerical model overestimates the measured moment for angles greater than 50° including the collapse moment, and it underestimates the collapse angle. The theory underestimates the measured moments up to about 100°, and then it overestimates the collapse moment and collapse angle. It may be concluded from Fig. 5 that the numerical model is reliable when the angle of bundle rotation is a sharp angle, but improvement is needed in the range of obtuse angles to consider a faster increase of angle with the applied moment.

C. Small-Scale Experiments

The numerical model was validated by comparisons to full-scale observations in the preceding two sections. However, the load shedding tests were carried out on a single line, whereas the bundle rotation was obtained during static tests. Therefore, the numerical model was also validated by simulating load shedding tests on the small-scale experimental twin bundle presented in Section II, and comparing the calculated and measured static sags of the loaded cable, the vertical components of cable vibration after the load sheds from one of the cables, and the angles of bundle rotation. Experiments were carried out with the two Vanguard cables whose properties are listed in Table 1. The static sag of the cables with diameters of 3.2 mm and 4.8 mm is increased by 3.7 cm and 1.5 cm, respectively, after attaching the loads. The same increments in the sag are 3.3 cm and 1.5 cm according to the numerical model. In Table 3, the results of the dynamic analysis implemented by the model are compared to experimental observations. These results were obtained for the cable of 3.2-mm diameter when loads shed suddenly from one

TABLE III
COMPARISON OF NUMERICAL AND EXPERIMENTAL RESULTS OBTAINED DURING VIBRATION FOLLOWING SHEDDING FROM EITHER CABLE WHEN THE OTHER ONE IS LOADED (CABLE WITH DIAMETER OF 3.2 MM), (A) JUMP HEIGHT OF SHEDDING CABLE AT MID-SPAN ABOVE LOADED POSITION, (B) RATIO OF JUMP HEIGHT OF SHEDDING CABLE IN TWIN BUNDLE (JH) AND JUMP HEIGHT OF SHEDDING SINGLE CABLE (JH$_{SINGLE}$), (C) MAXIMUM ANGLE OF BUNDLE ROTATION

Number of spacers	Jump height of shedding cable		
	Small-scale experiment (cm)	Small-scale model (cm)	Full-scale model (m)
0 (single cable)	18.9 / 21.4	16.1	4.085
2	13.3 / 14.4	11.6	2.88
4	9.0 / 9.7	8.2	2.09
1	4.8 / 5.2	4.8	1.23
3	5.5 / 5.5	5.0	1.76
5	5.4 / 5.5	5.0	1.70

(a)

Number of spacers	JH / JH$_{single}$ (%)		
	Small-scale experiment	Small-scale model	Full-scale model
2	67 – 70	72	71
4	45 – 48	51	51
1, 3, 5	24 – 29	30 – 31	30 – 43

(b)

Number of spacers	Maximum angle of rotation (deg)		
	Small-scale experiment	Small-scale model	Full-scale model
1	62 / 69	72	91
3	88 / 110	86	102
5	88 / 106	77	104

(c)

cable while the other cable remains loaded. Each shedding scenario was repeated twice with alternation of the cable which loads shed from, so that two numbers appear in the column "experiments" of Table 3. The cases when a spacer is attached at mid-span (odd number of spacers along the span), and when there is no spacer at mid-span (even number of spacers) must be discussed separately. The reason for this is that the jump height is significantly lower in the proximity of a spacer; and the highest jump usually appears in the middle of the sub-span which is closest to mid-span. This position falls mid-span for even number of spacers. However, the jump at mid-span is considerably reduced for odd number of spacers. Furthermore, bundle rotation was observed at mid-span by recording the movement of spacer attachment points; consequently, bundle rotation is not measured for even number of spacers when there is no spacer attached at that position.

Table 3 compares experimental and numerical results, namely the cable jump at mid-span above the loaded position and the maximum angle of bundle rotation during the vibration following shedding from either cable when the other one is loaded. It may be observed clearly that the jump height decreases by adding an even number of spacers, and that this jump height when there is a spacer at mid-span is nearly independent from the number of spacers along the span. The

magnitude of jump height is underestimated by 5 to 20 % by the model (see Table 3a). The tendencies according to the number of spacers are approximated closely by the numerical model. So, although the ratio of jump height of the shedding cable in the twin bundle to the jump height of a single shedding cable is overestimated by up to 20 %, the discrepancy is below 10% in most cases (see Table 3b). It should be noted that when the other cable is unloaded, the reduction in the severity of vertical vibration due to additional spacers is less considerable, because the mass and damping effect of the other cable in the bundle is significantly lower. It should also be noted that these ratios depend on other parameters, such as the shedding load weight, which were kept constant in the experiments.

Table 3 also shows the maximum angle during bundle rotation, which appears to be around 70˚ for one spacer. However, it may approach or even exceed 90° for three and five spacers. Thus, increasing the number of spacers will not reduce bundle rotation; contrarily, further connections between the cables in the bundle may help the shedding cable to move above the other one everywhere along the span. The probable explanation of this result lies in the fact that the relative motion of the two cables is non-uniform along the span. The greatest transverse and vertical displacements of the shedding cable appear close to the middle of the sub-span, which is far from the spacer where the angle is measured. However, when the number of spacers is increased, this relative motion becomes more uniform and the several connection points (spacers) between the two cables contribute to increasing the angle of rotation at mid-span. According to Sections IV.B and IV.C, the model behavior is similar concerning bundle rotation in small-scale and in full-scale lines. Since the maximum angle of bundle rotation for one spacer was a sharp angle in the experiments, the model provided a close prediction, but it underestimated the bundle rotation by 10-20% for three and five spacers when the bundle rotation approached or exceeded a right angle.

In Fig. 6, typical time histories of vertical displacement are compared with the results of the numerical model for the cases of even numbers of spacers when one cable is shedding and the other one is loaded. Also, an ice-load model by increasing the cable density proportionally with the ice-load weight as proposed by [7] was applied to these cases. It was used to verify whether the shedding of distributed loads can be simulated by the shedding of 8 point loads attached symmetrically along the span. The resulting vibration is slightly more severe with the point-loads model. However, the difference is not significant, e.g. the discrepancy between the jump heights is less than 5%. Considering that similar discrepancy also appears even between the two experimental results obtained under the same conditions, the approximation of distributed loads by point loads is satisfactory. Model predictions underestimate the jump height obtained experimentally by 10 to 20%, which is in accordance with the results listed in Table 3a. The reason for this difference probably lies in the simplification of suspension modeling. The
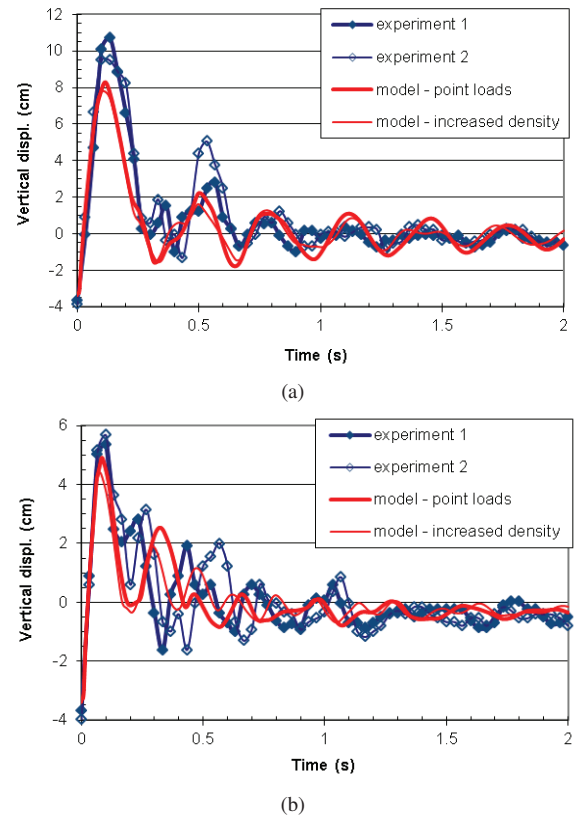

Fig. 6. Vertical vibration of shedding cable when the other one is loaded; experiment 1 and experiment 2: experimental results with shedding from cable 1 and cable 2, respectively, model – point loads: ice load considered by point loads, model – increased density: ice load considered by increased cable density [7]; (a) two spacers, (b) four spacers
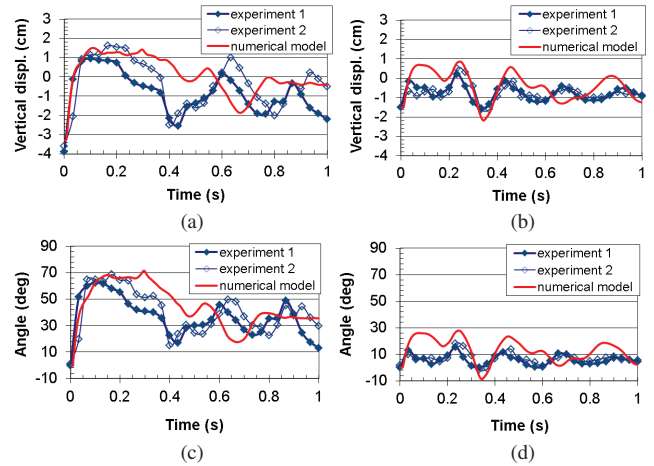

Fig. 7. Vertical displacement of shedding cable and angle of rotation of bundle with one spacer at mid-span following shedding from either cable when other one is loaded; (a) vertical displacement, cable with diameter of 3.2 mm, (b) vertical displacement, cable with diameter of 4.8 mm, (c) rotation angle, cable with diameter of 3.2 mm, (d) rotation angle, cable with diameter of 4.8 mm

underestimated cable jump could also be explained by an overestimated value for cable damping. The latter explanation is not probable, however, because the decay of vibration is closely predicted by the model. The period of the dominant vibration mode is 0.33 s when two spacers are applied, although the second peak is delayed in the experience, i.e. the

time between the first and second peaks exceeds 0.4 s (peaks at about 0.12 s and 0.55 s), whereas the time between the second and third peaks is less than 0.3 s (peaks at about 0.55 s and 0.8 s). Higher vibration modes are also present (see the smaller peaks in Fig. 6). Their amplitude is greater during the experiments. This is particularly the case when four spacers are applied along the span so that a single dominant vibration mode cannot be distinguished.

Fig. 7 presents typical time histories of the vertical displacement and rotation of bundle in the case of an odd number of spacers during the vibration following shedding from one cable while the other one is loaded. Fig. 7 compares the results of experimental measurements to those of numerical simulations. Furthermore, the effects of different cable diameters are also presented in this figure, because the same shedding scenarios were simulated using cables with two different diameters. Thus, according to Fig. 7, the model approximates closely the jump height of the shedding cable and the maximum angle of bundle rotation for the 3.2-mm diameter cable. The discrepancy between the computed and measured values is 15% or less. However, the model overestimates the jump height and the maximum angle for the 4.8-mm diameter cable. Possible explanations of this problem are (i) the measurement error of the cable stress-strain curve, as the model is specially sensitive for the initial tangent of that curve, or (ii) the underestimation of the cable damping. Further differences between the measured and calculated time histories, as presented in Fig. 7, are that the model underestimates the extent of drop after the first peak, so that the peaks following this drop are predicted about 0.1 s earlier as observed in the experiments for the 3.2-mm diameter cable. The comparison of Figs. 7a and 7b, as well as Figs. 7c and 7d, shows the great extent with which the increase in cable diameter reduces the jump height and maximum angle of bundle rotation. It should be clear, however, that the application of cables with greater diameters increases the load due to dead weight with the third power of cable diameter.

V. APPLICATION FOR A FULL-SCALE SPAN WITH A TWIN BUNDLE

The present model was used to simulate sudden ice shedding from the full-scale span of Bersfort conductors presented in [8], so that in addition to vertical cable vibration, bundle rotation was also simulated. The model considers one span with length of 200 m, including Bersfort conductors whose geometrical data are provided in Table 2. Its stress-strain curve is considered linear for positive strains with Young's modulus of 67.6 GPa, and no compression is allowed. Dead ends are assumed at the suspensions where the only free degree of freedom is the rotation around the axis perpendicular to the plane of structure. Each cable was simulated by 100 elements, and concentrated loads were applied at every fourth points. It was verified that increasing the number of loads along the span caused negligible differences in the results. The applied load corresponded to a load due to 50-mm-thick glaze

ice whose density is 900 kg/m^3. The damping ratio of the spacer was set at $\zeta_s = 0.2$ in correspondence with [17].

Tendencies similar to those obtained for the small-scale model were observed concerning the effects of the number of spacers on jump height and on the maximum angle of bundle rotation following ice shedding. The reduction in the ratio of jump height of the shedding cable in the twin bundle to the jump height of a single shedding cable due to additional spacers was similar to that observed in the small-scale tests (see Tables 3a and 3b). It should be kept in mind, however, that when the ice load is lower, the reduction in the jump height due to additional spacers is less considerable. Table 3c shows that after the shedding of high ice load (thickness of 50 mm) the maximum angle of rotation exceeded 90°, which increases significantly the risk of bundle collapse. The maximum angle of bundle rotation was greater for three and five spacers than for one spacer, which also corresponds to the tendency observed in the small-scale experiments.

VI. CONCLUSIONS

Cable vibration and bundle rotation following sudden ice shedding from either subconductor of a twin bundle have been simulated numerically and experimentally. The numerical model was validated by full-scale and small-scale experiments, and was applied to a full-scale span with a twin bundle. The full scale tests involved (i) load shedding from a single conductor where the conductor jump was studied and (ii) static torsional tests on twin bundles where the bundle rotation was observed. The small scale tests simulated different load shedding scenarios with up to five spacers along the span. The vertical component of cable vibration and the bundle rotation at mid-span were recorded and calculated. Similar scenarios were simulated, and the same parameters were determined when the model was applied to a full-scale twin bundle. The following conclusions are drawn from the results. The tendency of reduction in the cable jump height above the loaded position due to an increasing number of spacers along the span was predicted within 10 % by the model, although it approached 20% in some cases. The same discrepancies were observed between the numerically and experimentally obtained values for jump height. The maximum angle of bundle rotation was estimated satisfactorily for sharp angles. However, improvement to the model is needed by considering the configuration of the vibrating span more precisely for severe vibrations when the bundle rotation exceeds right angle. Increasing the number of spacers by up to four reduces the cable jump height significantly as compared to the jump height of the single cable. The application of a spacer at mid-span may lead to a further decrease in the cable jump, although in this case a greater jump may appear elsewhere. However, the bundle rotation cannot be reduced by increasing the number of spacers. The presented scenarios considered extreme cases when one subconductor sheds suddenly and fully, these results being useful to predict extreme dynamic effects. However, further tests and the corresponding modification of the

numerical model are recommended for future research in order to simulate more representative propagating shedding.

VIII. References

[1] V. T. Morgan, D. A. Swift, "Jump height of overhead-line conductors after the sudden release of ice loads," *Proc. of IEE*, vol. 111(10), pp. 1736-1746, 1964.

[2] O. Nigol, G. J. Clarke, D. G. Havard, "Torsional Stability of Bundle Conductors," *IEEE Trans. on Power Apparatus and Systems*, vol. PAS-96(5), pp. 1666-1674, 1977.

[3] Y. Matsubayashi, "Theoretical Considerations of the Twisting Phenomenon of the Bundle Conductor Type Transmission Line," Sumimoto Electric Technical Review (1), pp. 9-21, 1963.

[4] D. G. Havard, P. Van Dyke, "Effects of Ice on the Dynamics of Overhead Lines. Part II: Field Data on Conductor Galloping, Ice Shedding and Bundle Rolling," in. *Proc. 11th International Workshop on Atmospheric Icing of Structures*, Montreal, QC, Canada, pp. 291-296, 2005.

[5] A. Jamaleddine, G. McClure, J. Rousselet, R. Beauchemin, "Simulation of Ice Shedding on Electrical Transmission Lines Using ADINA," *Computers & Structures*, vol. 47(4/5), pp. 523-536, 1993.

[6] ADINA, *Theory and Modeling Guide*, Watertown, MA, 2004.

[7] M. Roshan Fekr, G., McClure, "Numerical modelling of the dynamic response of ice shedding on electrical transmission lines," *Atmospheric Research*, vol. 46, pp. 1-11, 1998.

[8] L. E. Kollár, M. Farzaneh, "Vibration of Bundled Conductors Following Ice Shedding," *IEEE Trans. on Power Delivery*, vol. 23(2), pp. 1097-1104, 2008.

[9] L. E. Kollár, M. Farzaneh, "Modeling the Dynamic Effects of Ice Shedding on Spacer Dampers," *Cold Regions Science and Technology*, vol. 57, pp. 91-98, 2009.

[10] ASTM A-370, "Standard Test Methods and Definitions for Mechanical Testing of Steel Products," Annual Book of ASTM Standards, Section One: Iron and Steel Products, vol. 01.03, pp. 102-150, 2004.

[11] L. Kempner Jr., "Longitudinal Impact Loading on Electrical Transmission Line Towers - A Scale Model Study," Ph.D. dissertation, Portland State University, Portland, OR, 1997.

[12] M. Roberge, "A Study of Wet Snow Shedding from an Overhead Cable," M.Eng. thesis, McGill University, Montreal, QC, 2006.

[13] L. E. Kollár, M. Farzaneh, "Dynamic behavior of cable systems with spacers following ice shedding," in *Proc. ICNPAA: Mathematical Problems in Engineering and Aerospace Sciences*, Budapest, Hungary, pp. 399-406, 2006.

[14] H. M. Irvine, *Cable Structures*, MIT Press: Cambridge, MA, USA, 1981.

[15] K.-J. Bathe, *Finite Element Procedures*, Prentice-Hall: Upper Saddle River, NJ, 1996.

[16] H. M. Irvine, T. K. Caughey, "The linear theory of free vibrations of a suspended cable," *Proc. R. Soc. Lond.* A 341, pp. 299-315, 1974.

[17] C. Hardy, P. Bourdon, "The influence of spacer dynamic properties in the control of bundle conductor motion," *IEEE Trans. on Power Apparatus and Systems*, PAS-99(2), pp. 790-799, 1980.

IX. Biographies

László E. Kollár received a M.Sc. degree in Mechanical Engineering from the Budapest University of Technology and Economics, Hungary in 1997, a Ph.D. degree in Mechanical Engineering from the same university in 2001, and a M.Sc. degree in Mathematics from the University of Texas at Dallas, USA in 2002.

In 2002, he joined CIGELE/INGIVRE at the University of Quebec at Chicoutimi as a Postdoctoral Fellow, where he currently is a Research Professor on grant. His research interests include theoretical and experimental modeling of atmospheric icing processes and ice shedding from cables. He previously worked on the modeling of controlled unstable mechanical systems with time delay.

Masoud Farzaneh (M'83-SM'91-F'07) is Director-founder of the International Research Center CENGIVRE, Chairholder of the CIGELE NSERC/Hydro-Quebec/UQAC Industrial Chair and of the INGIVRE Canada Research Chair related to power transmission engineering in cold climate regions. He authored or co-authored more than 500 technical papers, and 18 books or book chapters. Prof. Farzaneh has so far trained more than 100 postgraduate students and postdoctoral fellows. Actively involved with CIGRÉ and IEEE, he is Convenor of CIGRE WG B2.44 on coatings for protection of overhead lines during winter conditions, and member of the Executive Committee of CIGRE Canada. He is currently Administrative Vice-President of IEEE DEIS, and member of the Editorial Board of IEEE Transactions on Dielectrics and Electrical Insulation. He is Fellow of IEEE, Fellow of The Institution of Engineering and Technology (IET) and Fellow of the Engineering Institute of Canada (EIC). His field of research encompass high voltage and power engineering including the impact of cold climate on overhead transmission lines. His contributions and achievements in research and teaching have been recognized by the attribution of a number of prestigious prizes and awards at national and international levels.